Water retention curves of a dyke: in-situ vs laboratory determination

P.A. Mayor & S.M. Springman
Institute for Geotechnical Engineering, ETH Zurich, Zurich

W.F. Morales
formerly Institute for Geotechnical Engineering, ETH Zurich, Zurich; Geonumérica, SGA SAS, Bogota

ABSTRACT: An innovative field test has been carried out by creating a rectangular, piled cell around a section of an existing river dyke, which was heavily instrumented to measure meteorological inputs, pore pressure, volumetric water content and suction. The response of the dyke was studied while the water table was cycled through four distinct phases over 425 days to represent flood conditions, including a 3-day irrigation experiment. In-situ water retention curves were determined from field data at different points of the dyke and compared with water retention curves measured in unsaturated laboratory tests performed on specimens sampled from the dyke. The field and laboratory water retention curves differed substantially and are compared with computed curves derived from grain size distributions, and based on different empirical relationships. Each test or method predicts parts of the curves better than the other. The study indicates caution should be employed when using laboratory results for predicting field behaviour, or for the design of earthen structures. A combination of different determination methods can be used and calibrated against any data obtained, or simply the most appropriate method should be applied for field cases.

1 INTRODUCTION

Construction of flood defences was initiated in Switzerland in the late nineteenth century, effectively protecting the land for a period of more than a century (with only two major flood events > CHF 500M damage). These protection systems were no longer fit for purpose after 1977, since a higher frequency of events was accompanied by a notable increase in damage. Having been constructed before the birth of modern geotechnics, the existing dykes neither complied with the latest state of technology nor fulfilled the requirements of a modern flood defence system.

More advanced protection works had to be designed along many rivers, including the prediction of the dyke response under expected high water levels and the evaluation of the safety degree of the existing dykes, to establish priorities for remediation.

During planning of the third Rhone correction, a temporary test cell was constructed to observe and measure the response of a dyke to changes in water level of different heights and durations, which was controlled on the riverside through a pump system.

It was also possible to determine some of the unsaturated soil parameters in the field. These were compared with results from laboratory tests and predictions based on empirical relationships with the grain size distribution, to be able to simulate the dyke behaviour under the expected climatic changes.

2 FIELD TEST

2.1 *Field site and test cell*

A section of the Rhone river dyke was encapsulated within a sheet-pile box constructed from Larssen 25 pile sections of 11 m in length. This extended 12.5 m in the flow direction with a 33 m width perpendicular to the river. This was shortened by 9.3 m before the

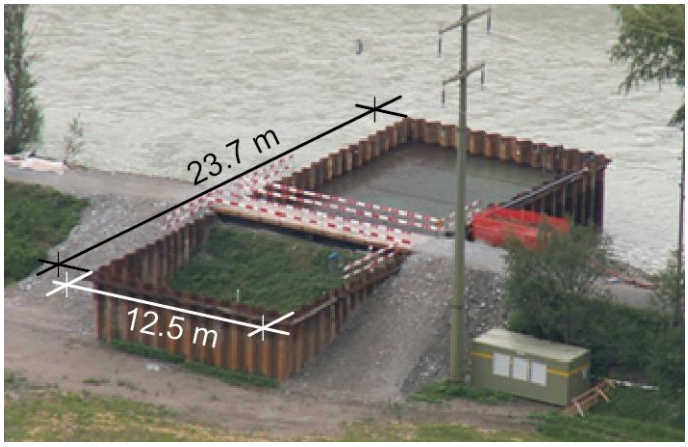

Figure 1. Aerial view of the dyke and the (shortened) test cell.

high water season, after the first test phase (Figure 1) to reduce the constriction of the river bed.

The levee is 3.3 m high above airside ground level at the test site. The lower part has been built during the first Rhone correction (1863-1894), mainly with material from the upper fluvial deposit, whereas the upper part is made of coarser material and has been added during the second correction (1930-1960).

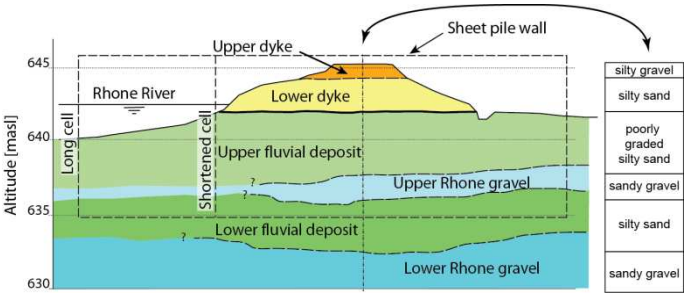

Figure 2. Geological cross section of the test site.

The levee is founded on an upper fluvial deposit, consisting mainly of silty fine sand. A layer of permeable upper Rhone gravel has been deposited under this layer and above a lower fluvial deposit, classified as SW-SM. The lower Rhone gravel, with classification varying from GW to SP, lies below.

2.2 *Instrumentation*

The main goal of the instrumentation was to investigate the dyke behaviour in the unsaturated zone. Suction and water content in the soil have been measured pairwise in the lower dyke at depth varying from 0.9 m to 1.5 m to determine the Water Retention Curve in the field.

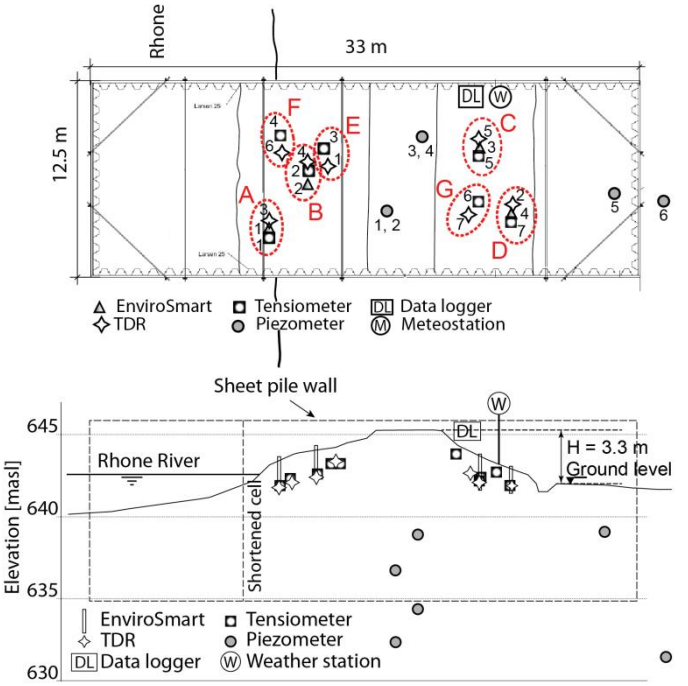

Figure 3. Layout of the instrumentation in the dyke.

Seven jet-fill tensiometers, equipped with electronic pressure transducers, have been installed to measure suction. The volumetric water content was monitored by means of 7 time domain reflectometers (TDR) and 4 EnviroSmart tubes (ESM), equipped with six water content gauges each. Four tensiometers were combined with both one TDR and one EnviroSmart (zones A, B, C and D in Figure 3). Each tensiometer in zones E, F and G, was combined with one TDR, giving a total of 11 pairs of suction and water content measurements in the lower dyke. Piezometers were located in and outside the cell at different depths to monitor the water table and the river level. A weather station recorded the meteorological conditions during the test, including air temperature, air humidity, air pressure, precipitation, wind speed and direction and sun radiation. Data were collected every 10 minutes, stored by means of a data logger, and downloaded on demand by a mobile phone link.

2.3 *Test history*

The test lasted 425 days (from April 2007 to June 2008) and consisted of four different phases (Figure 4). Several high water levels of different heights and durations were simulated during the first phase. The cell was then shortened and three long lasting high water periods were simulated. A sprinkling test was performed in the beginning of the third phase, directly followed by a long-lasting high water period.

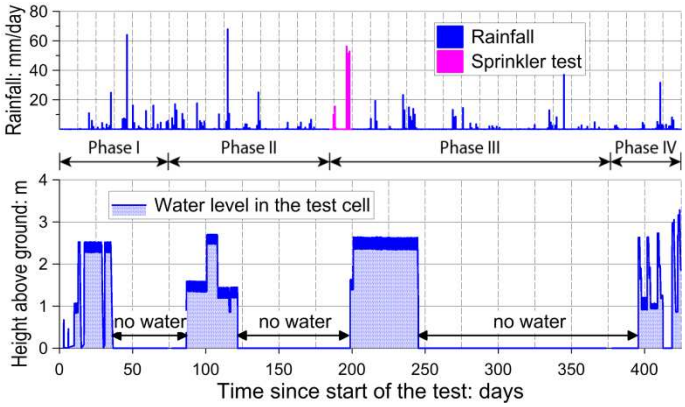

Figure 4. Test history (Ground level = 642 masl).

The dyke was then allowed to "recover" from early December to early May. The fourth phase of the test consisted of four consecutive high water levels with very short recovery periods in between, followed by an overtopping experiment.

The depth of the ground water level varied between 1.7 m and 3.5 m below surface during the duration of the test. This more or less followed the fluctuation of the river level, but at a height of about 2 m below.

2.4 *Dyke behaviour*

The behaviour of the dyke during the test on the water side is illustrated in Figure 5 with the evolution of the water content measured by the EnviroSmart 2 device, with sensors situated at a depth of 0.19 (ESM2.1), 0.39, 0.59, 0.79, 1.09, 1.39 (ESM2.6) m below the surface.

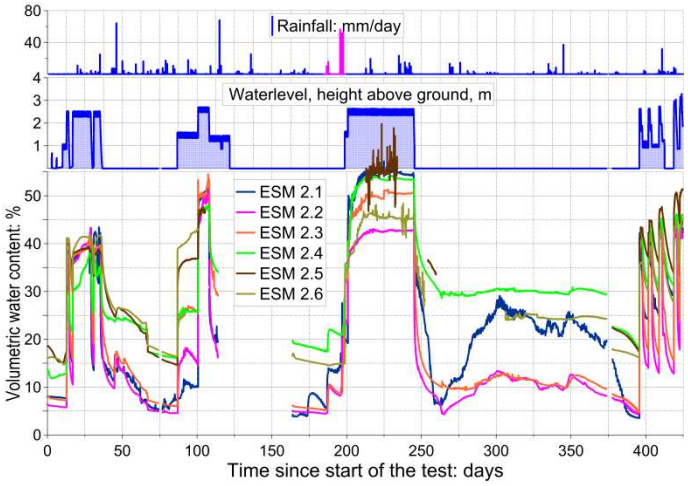

Figure 5. Dyke response, EnviroSmart 2 (water side).

The water content increased rapidly as soon as the water level reached the elevation of the sensors. The three upper sensors also reacted quickly after the drop in the cell water level, whereas the three lower sensors recovered more slowly from the high water, remaining close to the highest level reached, even after the long pause following the high water period during Phase III. This behaviour was attributed to lower permeability in Zone B of the dyke.

Data are missing due to the failure of some sensors, caused by infiltration of water into the EnviroSmart tube, which was lying under water at that time. Phase IV also shows an increase in the maximum water content, showing that achieving full saturation is also a function of the seepage time.

EnviroSmart 3, with sensors situated at depths of 0.22 (ESM3.1), 0.52, 0.82, 1.12, 1.52, 1.92 (ESM3.6) m below the surface, illustrates the dyke behaviour on the air side (Figure 6). The high water level in the cell during phase I had no influence on the water content of the dyke on the air side. Heavy rainfall (63 mm in a day) caused an increase in the water content of about 15% at the sensor located at 0.22 m depth, with a strongly decreasing effect with depth.

The four lower sensors, beginning with the deepest one, showed a clear increase of the water content after the water level rose by 2.8 m above ground in Phase II. However, once the water level was reduced in the cell, the water content dropped quickly and reached the original value at the end of Phase II.

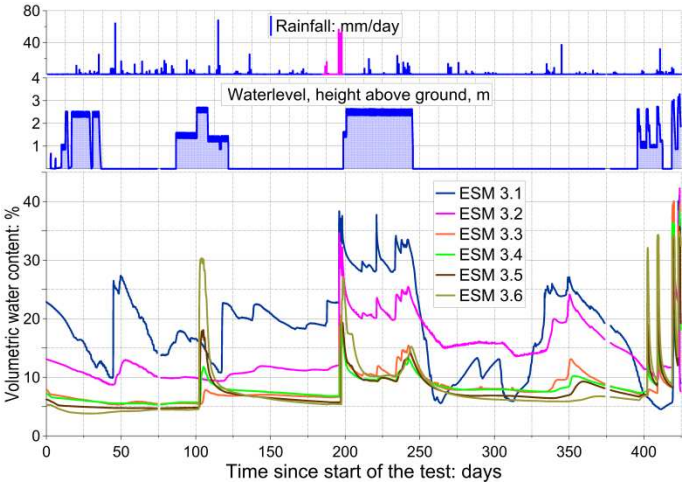

Figure 6. Dyke response, EnviroSmart 3 (air side).

All sensors, from the top downwards, reacted to the sprinkler test at the start of Phase III. Subsequent rain events continued to influence the water content. The measured values remained higher during the high water level period in the cell, decreasing quickly after the water level dropped. The dyke is more permeable here than on the waterside at EnviroSmart 2. A water content corresponding to, or near, saturation was reached (on the air side) only in Phase IV, after having been submitted to four consecutive high water cycles up to the crest of the dyke.

3 WATER RETENTION CURVES

Determination of the Water Retention Curve (WRC) in either the field or in the laboratory exhibits significant differences and is demanding, time consuming and expensive. Alternative methods based on basic geotechnical properties have been developed. In this study, in addition to the field and laboratory tests, the WRC are computed by two methods derived from the soil grain size distribution (GSD), the Arya and Paris method (Arya & Paris, 1981) and the Modified Kovács method (Aubertin et al., 2003).

3.1 *Field tests*

The initial drying curve (Pham et al., 2005) cannot be determined in a field test because the initial soil stress state is variable inside the dyke. However the main (boundary) drying / wetting curves can be estimated by measuring repeated drying and wetting cycles.

The field test being a transient process, continuous measurements are needed to register the dyke's response. Results of the combined measurements of volumetric water content and suction for the determination of the WRCs are shown for the water side (zones A, B, F and E) in Figure 7. Hysteretic response of the WRC, differences in the time response of the

various types of sensors, changing temperature during the test or a loss of saturation in the tensiometers, especially during phase I, help to explain some of the scatter in Figure 7.

Some limitations of the field test had to be taken into account for the determination of the field WRCs. Measuring rates (every 10 minutes) were insufficient to capture the wetting curve accurately, so only values obtained during the drying phases were considered. High water contents were reached on the air side of the dyke only during test phase IV, making it impossible to determine a full WRC in the phases I to III. Therefore, all WRCs were determined based on the measurements from test phase IV. The resulting water retention curves were then determined for every measurement pair: see the maximum water content at θ_u and the air entry value Ψ_{AEV} in Figure 8.

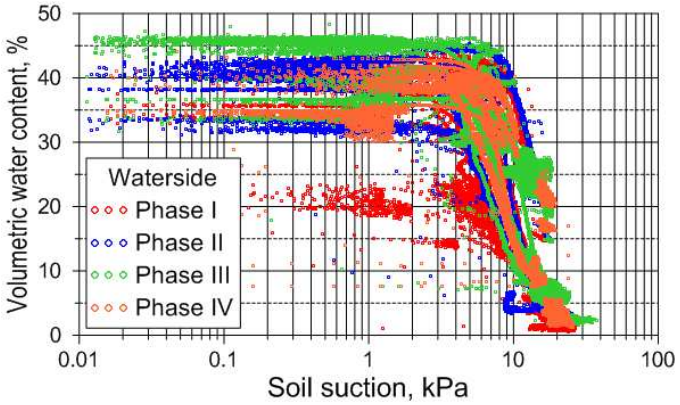

Figure 7. Water content – suction measurements (water side).

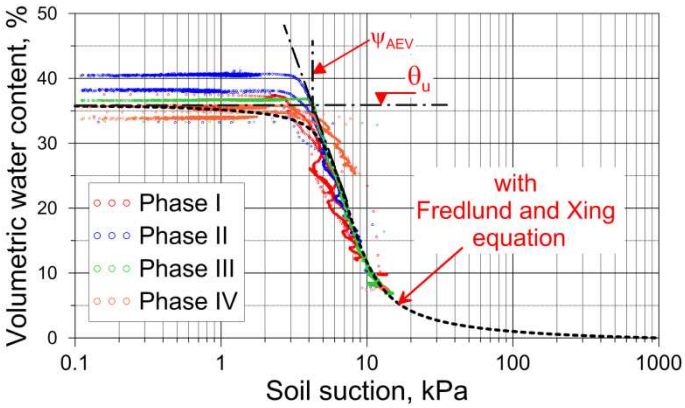

Figure 8. WRC at Point A, Determination of θ_u and air entry value (Ψ_{AEV}).

As most of the measured minimum water contents were higher than the residual water content, the WRCs were extrapolated to the residual zone using Fredlund and Xing's equation (1994) with a correction factor for the suction range beyond the residual value (Figure 8). This procedure has been repeated for all measured pairs of water content and suction, giving eleven WRCs, as summarised in Figure 9.

With the exception of the two WRCs obtained for Zone B (Figure 3), which show a higher range of suctions, the WRCs measured in the field lie in a narrow range. These results confirm that zone B exhibits a different, and less representative, response than the rest of the dyke.

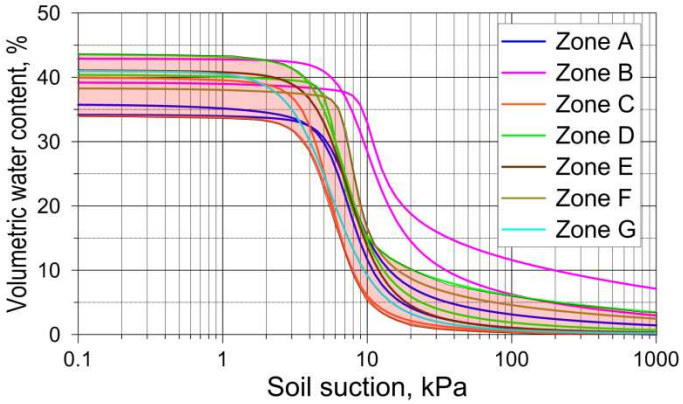

Figure 9. Field Water Retention Curves with scatter zone.

3.2 *Laboratory tests*

The WRCs of specimens sampled from different locations in the lower dyke were determined on reconstituted samples, in the Fredlund apparatus by Morales et al. (2011) and in Tempe cells by Lustenberger (2014), at densities covering the density range observed in the field test.

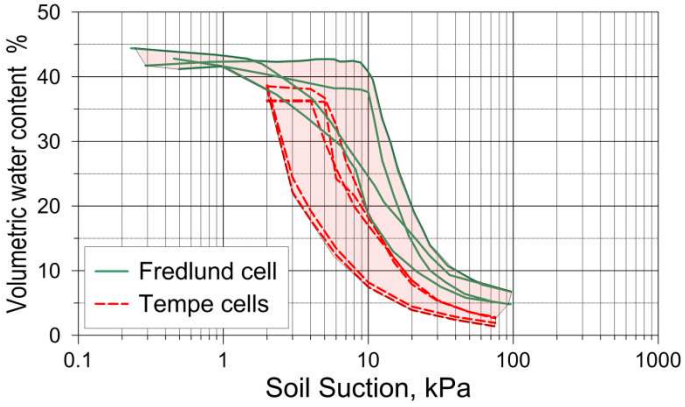

Figure 10. Laboratory water retention curves.

The first test in the Fredlund Cell was conducted through both the drying and wetting paths at void ratio e = 0.75 and an overburden pressure (σ_v) of 40 kPa; the second one at e = 0.72 and σ_v = 80 kPa. Five tests have been conducted along the drying path in the Tempe cells, at void ratios varying from e = 0.81 to e = 0.98. The specimens in the Tempe cell being unloaded, lower e values could not be tested. Results of the laboratory tests are summarised in Figure 10.

3.3 *Computed from grain size distribution (GSD)*

The Arya & Paris method proposed by Arya and Paris (1981) and the Modified Kovács method proposed by Aubertin et al. (2003) are used here.

3.3.1 *Grain size distributions*

Specimens were all taken from the lower dyke. The 4 GSDs of the specimens tested in the laboratory were used to predict the laboratory WRC. A further 7 GSDs obtained from the dyke specimens were used to predict the field WRC (Figure 11). No specimens were plastic. Classification ranges from SM (7 samples) to SP-SM (2 samples).

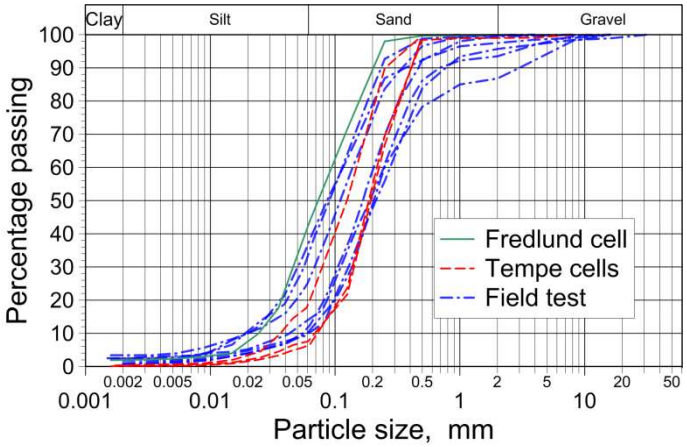

Figure 11. Grain size distributions from field / laboratory tests.

3.3.2 *Arya and Paris (A&P) method (1981)*

The A&P-method uses the complete GSD to calculate the WRC, and some empirical factors to account for uncertainties in the procedure. A value of 1.30 was chosen for the factor α. Figure 12 shows the computed WRCs, calculated with the A&P-method for the GSD of both the laboratory and the field samples. The void ratios of the different tests were used for the calculation of the laboratory WRCs. Values of e = 0.818 and e = 0.667 were taken for the field case (corresponding to porosities of n = 0.45 and n = 0.40).

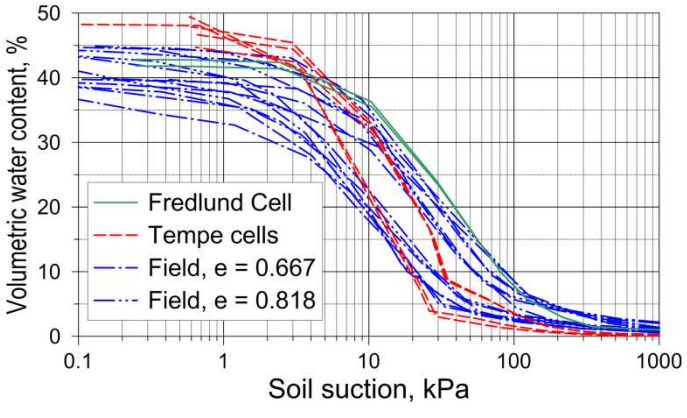

Figure 12. Computed WRCs of the laboratory and field samples using the A&P-method.

3.3.3 *Modified Kovács (MK) method (2003)*

The MK-method needs D_{10} (diameter corresponding to 10% passing the GSD), C_u (coefficient of uniformity $C_u = D_{60}/Dd_{10}$) and the void ratio e, as input parameters. The same void ratios were assumed as for the A&P-method. Figure 13 shows the computed WRCs calculated with the MK-method for the GSD of the laboratory and field samples.

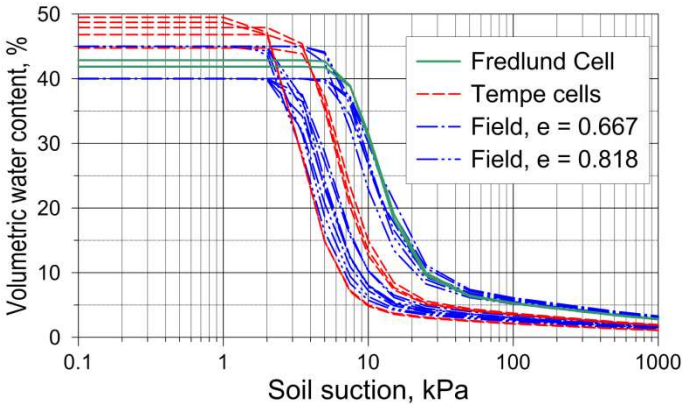

Figure 13. Computed WRCs of the laboratory and field samples using the MK-method.

4 COMPARISON WITH THE FIELD RESULTS

The field test carried out during planning of the third Rhone correction gave an excellent (and rare) opportunity to compare water retention curves measured in the field with those measured in the laboratory and those computed through the A&P and MK methods.

4.1 *Field vs. laboratory*

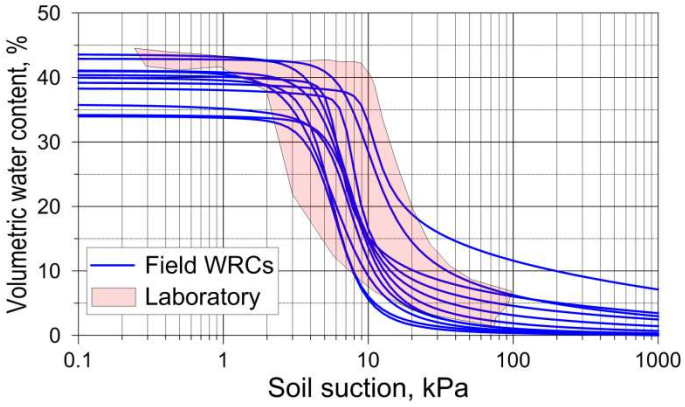

Figure 14. Field WRCs vs scatter zone of the laboratory test.

Figure 14 shows the field WRCs with the scatter zone of the laboratory tests. Combining data from tests from the Fredlund cell with data from the Tempe cell tests, values are quite consistent with the measured WRC. The zone of the measured air entry values lies completely in the scatter zone of the laboratory test.

The laboratory curves slightly overestimate the measured field values in the zone of the residual water content.

This result was only possible by combining tests in the Fredlund cell with tests in Tempe cells. A much less satisfactory result (see Figure 10) would have been achieved using only one of these methods.

4.2 *Field vs Arya & Paris method*

The field WRCs are plotted in Figure 15 together with the scatter zone of the WRC computed with the A&P-method based on the GSD of the field specimen. The A&P-method is in very good accordance with the measured curves in the zone of low suction up to the air entry value. The slope of the computed curves are less steep at suctions higher than the air entry value, and the water content was overestimated in comparison with the field results.

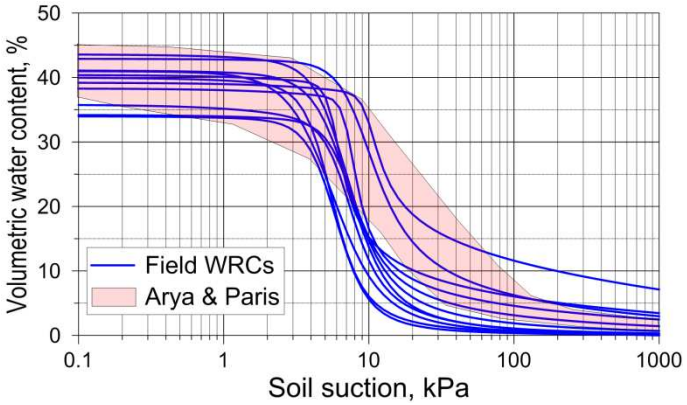

Figure 15. Field WRCs vs Arya & Paris method, $\alpha = 1.30$.

4.3 *Field vs Modified Kovacs method*

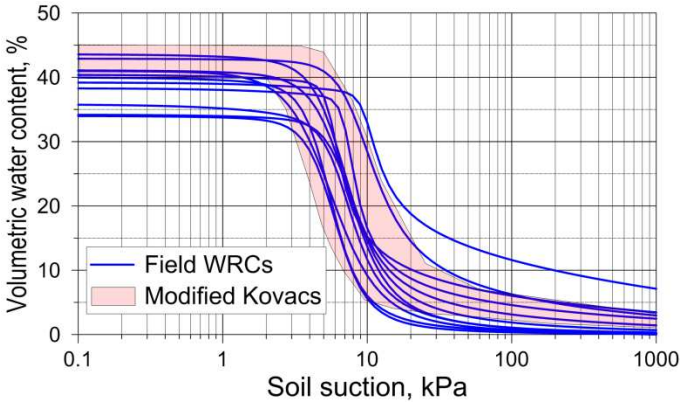

Figure 16. Field WRCs vs Modified Kovacs method.

The field WRCs are plotted in Figure 16 together with the scatter zone of the WRCs computed with the MK-method, which is in very good accordance with the measured WRCs in the zone between the air entry values and the residual zone. The maximum water content at low suction is only dependent on the assumed void ratios, giving a less satisfactory result than the A&P-method.

5 CONCLUSIONS

The results of the determination of Water Retention Curves are presented from measurement in a field test, in the laboratory and through prediction with two different methods based on soil grain size distributions. Comparing the results of the laboratory tests and of the computed curves with the field WRCs, it is obvious that each test or method predicts certain parts of the curves better than the other. However, considering the differences between the boundary conditions in the field and in the laboratory, the scatter in the GSD and void ratio of the dyke material, the accordance between measurements and predictions remains quite good. Based on the results of this study, it is recommended to combine a range of tests in the laboratory with different prediction methods (based on basic geotechnical properties) to achieve the best possible representation of volumetric water content as a function of suction.

6 ACKNOWLEDGEMENTS

The authors extend grateful thanks to the 3rd River Rhone Regulation Project, under which the field test was carried out.

7 REFERENCES

Arya, L.M. & Paris, J.F. 1981. A physicoempirical model to predict the soil moisture characteristic from particle-size distribution and bulk density data. *Soil Sci. Soc. of America J.*, 45(6): 1023-1030.

Aubertin, M., Mbonimpa, M., Bussière, B. & Chappuis, R.P. 2003. A model to predict the water retention curve from basic geotechnical properties. *Can. Geot. J.*, 40: 1104-1122.

Fredlund, D.G. & Xing, A. 1994. Equations for the soil-water characteristic curve. *Can. Geot. J.*, 31(4): 521-532.

Lustenberger, M., 2014. Wasserretentionskurve und Durchlässigkeitsfunktion siltig-sandiger Flussablagerungen, Master Thesis ETH, (unpublished).

Mayor, P.A., Springman, S.M. & Teysseire, P. 2008. In situ field experiment to apply variable high water levels to a river levee. *Unsat. Soils. Advances in Geo-Eng. (eds. D.G. Toll, C.E. Augarde, D. Gallipoli, S.J. Wheeler)*: 947-952.

Morales, W.F., Mayor, P.A., Springman, S.M. & Vogel, A. 2011. In-situ and laboratory water retention characteristics in a silty sand dyke. *Proc. of 15th Euro.Conf. on Soil Mech. and Geotech. Eng., A. Anagnostopopulos et al. (Eds):* 641-646.

Pham, H.Q., Fredlund, D.G. & Barbour, S.L. 2005. A study of hysteresis models for soil-water characteristic curves. *Can. Geotech. J.*, 42: 1548-1568